JOURNAL OF VIROLOGY, May 1985, p. 598–607
0022-538X/85/050598-10$02.00/0

Vol. 54, No. 2

Mass and Molecular Composition of Vesicular Stomatitis Virus: a Scanning Transmission Electron Microscopy Analysis

DANIEL THOMAS,[1]† WILLIAM W. NEWCOMB,[2] JAY C. BROWN,[2] JOSEPH S. WALL,[3] JAMES F. HAINFELD,[3] BENES L. TRUS,[4] AND ALASDAIR C. STEVEN[1]*

Laboratory of Physical Biology, National Institute of Arthritis, Diabetes, Digestive and Kidney Diseases[1] and Division of Computer Research and Technology,[4] National Institutes of Health, Bethesda, Maryland 20205; Department of Microbiology, University of Virginia School of Medicine, Charlottesville, Virginia 22908[2]; and Biology Department, Brookhaven National Laboratory, Upton, New York 11973[3]

Received 18 October 1984/Accepted 14 January 1985

Dark-field scanning transmission electron microscopy was used to perform mass analyses of purified vesicular stomatitis virions, pronase-treated virions, and nucleocapsids, leading to a complete self-consistent account of the molecular composition of vesicular stomatitis virus. The masses obtained were 265.6 ± 13.3 megadaltons (MDa) for the native virion, 197.5 ± 8.4 MDa for the pronase-treated virion, and 69.4 ± 4.9 MDa for the nucleocapsid. The reduction in mass effected by pronase treatment, which corresponds to excision of the external domains (spikes) of G protein, leads to an average of 1,205 molecules of G protein per virion. The nucleocapsid mass, after compensation for the RNA (3.7 MDa) and residual amounts of other proteins, yielded a complement of 1,258 copies of N protein. Calibration of the amounts of M, NS, and L proteins relative to N protein by biochemical quantitation yielded values of 1,826, 466, and 50 molecules, respectively, per virion. Assuming that the remaining virion mass is contributed by lipids in the viral envelope, we obtained a value of 56.1 MDa for its lipid content. In addition, four different electron microscopy procedures were applied to determine the nucleocapsid length, which we conclude to be 3.5 to 3.7 μm. The nucleocapsid comprises a strand of repeating units which have a center-to-center spacing of 3.3 nm as measured along the middle of the strand. We show that these repeating units represent monomers of N protein, each of which is associated with 9 ± 1 bases of single-stranded RNA. From scanning transmission electron microscopy images of negatively stained nucleocapsids, we inferred that N protein has a wedge-shaped, bilobed structure with dimensions of ~9.0 nm (length), ~5.0 nm (depth), and ~3.3 nm (width, at the midpoint of its long axis). In the coiled configuration of the in situ nucleocapsid, the long axis of N protein is directed radially, and its depth corresponds to the pitch of the nucleocapsid helix.

The basic features of vesicular stomatitis virus (VSV) structure are now reasonably well understood (2, 29, 46). The virion is cylindrical with a hemispherical cap at one end, giving the particle its characteristic bullet shape. Intact virions are approximately 70 nm in diameter and 180 nm long (27). They are composed of an internal "skeleton" structure surrounded by a lipoprotein envelope. The skeleton contains two major proteins (M and N) and two minor proteins (L and NS) in addition to the viral RNA. The envelope is composed of the virus-coded glycoprotein (G protein) and lipids derived from the host cell plasma membrane. The glycoprotein molecules form spikes which protrude outwards from the virion surface (19, 20, 22). "Nucleocapsid" complexes may be extracted from the virions. These complexes are strands consisting of the genome RNA tightly associated with N protein molecules which are closely packed along its length, together with some L and NS proteins. In intact skeletons, the nucleocapsid is associated with M protein and is coiled 30 to 35 times to form a helix with almost the same length as the virion (31).

Despite a sound qualitative understanding of VSV composition, considerable uncertainty persists concerning the quantitative aspects essential to a detailed understanding of the structure and assembly of the virion. Estimates of the content of N protein, for instance, range between 1,000 and 2,300 molecules per virion (3, 6, 27); for M protein the range is between 1,600 and 4,700 molecules, and similarly wide ranges of estimates have been reported for the other three viral proteins (2, 3, 6). Measurements of the virion RNA content have indicated that RNA accounts for between 0.7 and 3.0% of the total VSV mass (3, 6, 24). From these data, values of 122 to 525 megadaltons (MDa) can be calculated for the particle weight of native VSV. This range includes the values of 290 (14) and 355 MDa (48) obtained by the indirect technique of laser light scattering from suspensions of purified virions.

Recent advances in use of the scanning transmission electron microscope (9) have provided a method very well suited for measuring the masses of macromolecular particles in the size range of viruses (11, 18, 25, 37, 43, 44, 47). This technique allows the determination of individual particle masses by integrating the electron scattering from all parts of unstained specimens represented in digital images.

We report here the results of experiments in which the Brookhaven scanning transmission electron microscope (47) was used to determine the molecular weights of purified VSV and of two related structures, nucleocapsids and "shaved" virions from which the glycoprotein spikes have been enzymatically removed (7, 26). Companion experiments embracing a variety of electron microscopy techniques have been performed to determine the distribution of

* Corresponding author.
† Present address: Groupe de Recherche de Biologie Cellulaire, Centre National de la Recherche Scientifique, N°256, Universite de Rennes, Campus de Beaulieu, 35042 Rennes Cedex, France.

N protein subunits along the nucleocapsid and to verify earlier estimates of its total length (29). Taking into account relative protein abundances from biochemical analyses, we can interpret the scanning transmission electron microscopy (STEM) mass data in terms of absolute numbers of molecules per particle. The precision of these calculations is enhanced by the availability of molecular-weight values for the various proteins deduced from their recently determined primary sequences (12, 35, 40). Thus, our results lead to a fully specified account of the molecular composition of the vesicular stomatitis (VS) virion.

MATERIALS AND METHODS

Virus growth, purification, and digestion with pronase. All experiments were carried out with the Mudd-Summers strain of VSV (Indiana), which was grown on monolayer cultures of BHK-21 cells as described previously (31). For some experiments, virus proteins were radioactively labeled by including 5 μCi of L-[^{3}H]leucine (60 Ci/mmol; Amersham Corp., Arlington Heights, Ill.) per ml of the virus growth medium. The virus was purified from infected-cell medium by the method of Hunt and Wagner (16), modified so as to avoid pelleting the virus particles. Infected-cell medium was clarified by low-speed centrifugation (1,000 × *g* for 15 min), and virus was recovered from the clarified medium by ultracentrifugation in 6-ml portions on 30-ml linear sucrose gradients (10 to 30%) containing 10 mM Tris-HCl buffer (pH 7.4). Gradients were centrifuged for 120 min at 18,000 rpm (45,000 × *g*) in a Beckman SW28 rotor operated at 4°C. After centrifugation, the single band of virus material was harvested from gradients with a Pasteur pipette and dialyzed overnight at 4°C against 10 mM Tris-HCl (pH 7.4).

Glycoprotein spikes were removed from VSV by pronase treatment of intact virions (26). Solid pronase (Calbiochem-Behring, La Jolla, Calif.) was added directly to the clarified infected-cell medium to give a final concentration of 1 mg/ml. Digestion was allowed to proceed for 30 min at 37°C before treated virions were recovered by sucrose density gradient ultracentrifugation and dialysis as described above.

Nucleocapsid preparation. VSV nucleocapsids were prepared by detergent–high-salt extraction of purified virions (10). Dialyzed virus prepared as described above, at 4°C and a concentration of 0.5 mg/ml, was mixed with an equal volume of ice-cold 10 mM Tris-HCl (pH 8.5)–10% glycerol–1 M NaCl–2% Triton X-100. The disrupted virus was kept on ice for 10 min. The resulting clear solution was layered over a 1-ml pad of 100% glycerol in an SW50.1 ultracentrifuge tube and centrifuged at 35,000 rpm (120,000 × *g*) for 3 h at 4°C. The nucleocapsids, which formed a band just below the top of the glycerol pad, were recovered with a Pasteur pipette and dialyzed overnight at 4°C against 10 mM Tris-HCl (pH 7.4) before analysis by STEM or sodium dodecyl sulfate-polyacrylamide gel electrophoresis (SDS-PAGE).

SDS-PAGE. One-dimensional SDS-PAGE was carried out on 12.5% polyacrylamide slabs (10 by 18 cm, 2 mm thick) by using the stacking gel and buffer system described by Carroll and Wagner (5). Developed gels were stained with Coomassie blue and destained as described by Nagpal and Brown (28). The distribution of radioactive label on developed gels was determined by cutting the gel into 1-mm slices, which were counted in a liquid scintillation counter as described by Hunt and Brown (17).

STEM. STEM images were recorded at the Brookhaven Biotechnology Resource as described previously (25, 47) by using a 40-kV electron probe focused to a diameter of 0.25 nm. Images were recorded directly in digital form, with parallel acquisition of two dark-field images (each 512 by 512 pixels) from the small-angle (15 to 40 mrad) and large-angle (40 to 200 mrad) detectors. During observation the specimens were maintained at −150°C on a liquid N_2-cooled stage.

Unstained specimens were prepared by freeze-drying at a constant sublimation rate over a period of 6 to 8 h by a previously described procedure (25). The substrate was a carbon film (~2.5 nm thick) supported on a fenestrated thick-carbon support, which had previously been glow discharged in N_2. The sample was injected into a drop of buffer (previously applied to the grid) and allowed to adsorb for 10 min. Tobacco mosaic virus was added, and the grids were washed for three cycles with ammonium acetate (10 mM; pH 7.5) and then freeze-dried (25).

Preparations of negatively stained nucleocapsids were also examined by STEM by using a composite image of the bright-field signal minus twice the dark-field signal from the large-angle detector. After adsorption to a thin carbon film, the specimens were rinsed with ammonium acetate (10 mM, pH 7.4) and stained with uranyl sulfate (2%) or phosphotungstic acid (2%).

Analysis of digital data. The images were analyzed with a VAX 11/780 computer, a Gould DeAnza IP 8500 image processor, and the PIC software system (45; cf. reference 42). For mass measurements, the signal from the large-angle detector was used. Particles were selected interactively from images displayed on a television monitor; the designated subimages were then integrated to yield the mass measurements after background subtraction (13, 43, 44).

To reduce the experimental uncertainty in mass measurements of spread nucleocapsids caused by background fluctuations (see below), a program was developed to minimize the area of background included in the two-dimensional mass integral, while ensuring that the entire particle was included. According to this procedure, a displayed nucleocapsid image was broken up into segments enclosed in a succession of adjoining parallelograms specified interactively on the overlay plane of the video frame buffer by an operator using a graph pen-and-tablet system. A local background subtraction was applied to the contribution of each parallelogram in calculating the total mass integral. In each case, background values applicable to particular locations in the image field were computed as described previously (13).

Conventional transmission electron microscopy. Preparations of nucleocapsids were examined by conventional transmission electron microscopy with a JEOL 100 CX or a Philips EM400T electron microscope operated at 80 kV. After adsorption for 1 min on carbonized collodion-coated grids, specimens were washed with distilled water (two times for 20 s) and stained with a 5% aqueous solution of uranyl acetate. After 2 min the excess fluid was removed, and the grid was allowed to dry.

Images of well-extended nucleocapsids were recorded at a calibrated magnification of ×15,000. These negatives were then printed at a final magnification of ×41,400. Particle lengths were measured with a digitizer linked to a Zilog MCZ microcomputer by following the contour lengths of the nucleocapsids with a cross-hair cursor.

RESULTS

STEM mass determination of VSV and subviral particles. The relationship between the signal recorded by the STEM large-angle dark-field annular detector and the mass present

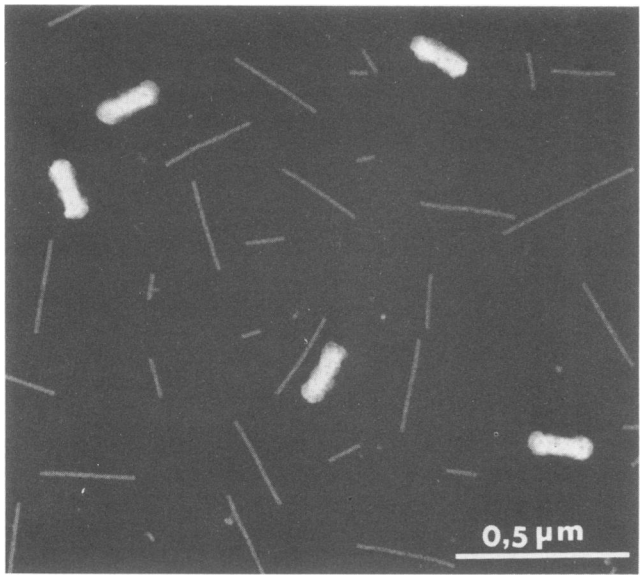

FIG. 1. STEM dark-field image of unstained freeze-dried VS virions. The VSV particles are characterized by their typical bullet shape and high image intensity (represented here as white). The rodlike particles are tobacco mosaic virus particles which were employed as internal mass standards.

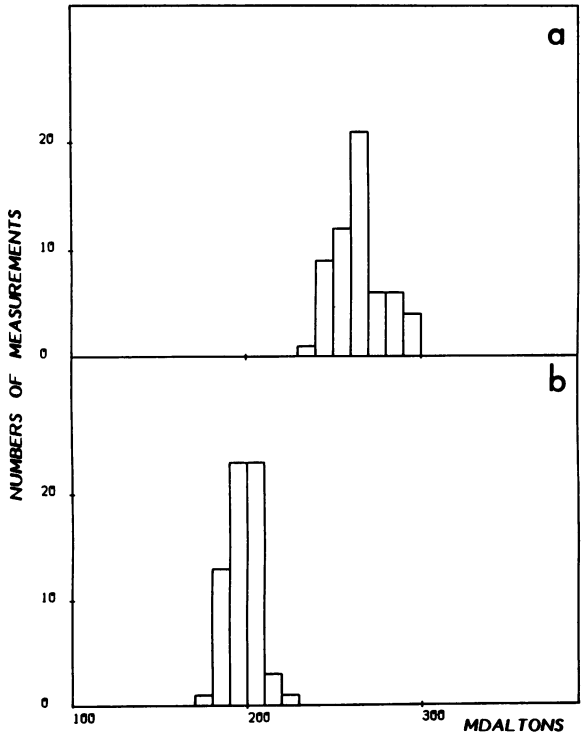

FIG. 2. Histograms showing the distributions of particle masses determined for (a) purified VS virions (n = 59) and (b) pronase-treated virions (n = 64).

in the sampled portion of the specimen may be exploited for direct mass determinations of individual particles from electron images of unstained specimens (11, 25, 43). The contributions from all parts of a particle were integrated after appropriate subtraction of the background contributed by the carbon support film and then calibrated relative to an internal mass standard, in this case tobacco mosaic virus (see above). Both VS virions and pronase-treated virions represent relatively thick specimens. Therefore, these images were transformed mathematically, by the procedure of Steven et al. (43), to compensate for nonlinearity caused by incipient multiple scattering of electrons. No such compensation was necessary for the relatively thin masses projected by spread nucleocapsids.

(i) VS virions. A typical dark-field STEM image of unstained VS virions is shown in Fig. 1. The VSV particles are characterized by their typical bulletlike shape and high image intensity relative to the tobacco mosaic virions. Such images formed the basis of the mass measurements compiled in Table 1. After we combined the mutually consistent results from two sets of experiments, a mean virion mass of 265.6 ± 13.3 MDa was obtained. The distribution of these measurements is represented in Fig. 2a. Calculations made directly from images which had not been compensated for the nonlinearity associated with multiple scattering yielded an average mass for the VS virion of 248.2 MDa, a 7% underestimate.

TABLE 1. STEM mass measurements of VS virions and subviral particles

Particle	Expt.	Mass (MDa)[a]	Average mass (MDa)[a]
Native virions[b]	1	271.6 ± 17.7 (17)	265.6 ± 13.3 (59)
	2	263.2 ± 10.1 (42)	
Pronase-treated virions[b]	1	197.8 ± 8.7 (51)	197.5 ± 8.4 (64)
	2	196.6 ± 6.1 (13)	
Nucleocapsids	1	70.5 ± 5.5 (36)	
	2	68.3 ± 4.5 (25)	69.4 ± 4.9 (72)
	3	68.3 ± 3.8 (11)	

[a] The number of determinations is shown in parentheses.
[b] Compensated for nonlinearity in the STEM dark-field signal caused by incipient multiple electron scattering (43).

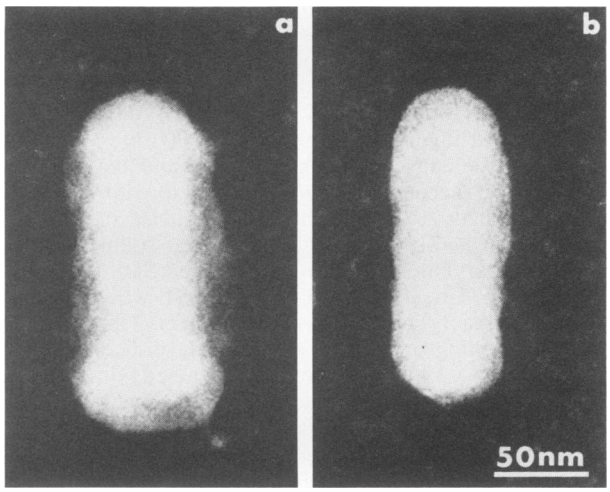

FIG. 3. High-magnification STEM dark-field images of an unstained VS virion (a) and a pronase-treated virion (b), which has a notably smooth periphery in contrast to the irregular edges of the native virion.

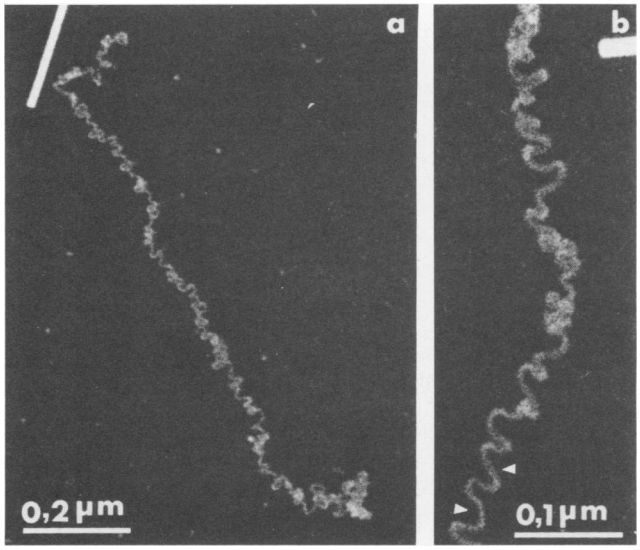

FIG. 4. STEM images of purified VSV nucleocapsids. The isolated nucleocapsid (a) has an irregular, serpentine appearance. Relatively short tracts of uniformly spread nucleocapsid strands (b, arrows) were used to perform local measurements of mass per unit length.

(ii) Pronase-treated virions. A similar mass analysis was conducted with images of pronase-treated (shaved) virions (Table 1 and Fig. 2b). The effect of proteolytic digestion on the virion morphology is illustrated in Fig. 3. The shaved particle (Fig. 3b) has a smooth clean-cut periphery in contrast to the rather irregular, ragged edges of the reference particle (Fig. 3a). Pronase-treated virions also had a reduced overall width of 63.5 ± 7 nm (n = 16) compared with 82 ± 8 nm (n = 22) for the native virion.

Two sets of shaved virions were analyzed. One had been treated with 1.0 mg of pronase per ml and the other with 0.5 mg of pronase per ml. Particles from the two preparations yielded indistinguishable mass values of 197.8 ± 8.7 and 196.6 ± 6.1 MDa, respectively (Table 1), indicating that the proteolytic digestion was complete in each case. The global average of these measurements, 197.5 MDa, shows a loss in mass of 68.1 MDa from the virion as a result of the pronase treatment. With the shaved-virion images, the kinetic (i.e., linear) approximation would have resulted in an underestimate of their mass by 5.8% (Table 1).

(iii) Nucleocapsids. STEM images of purified nucleocapsids are presented in Fig. 4. The nucleocapsids have an irregular, serpentine appearance and are spread out to various degrees (Fig. 4a). The densities they project are markedly lower than those of the tobacco mosaic calibration particles, in contrast to the situation with virions and shaved virions. With a spread nucleocapsid, a relatively low amount of total mass is distributed over a substantial area. Consequently, statistical fluctuations in the (dominant) contribution of the carbon film background to the signal are a major source of uncertainty in mass measurements. To minimize this effect, a computer program was specifically developed to demarcate the boundaries of such irregularly shaped particles (thus defining the areas to be integrated) to minimize the included areas of extraneous background (see above).

In an initial analysis, mass measurements were made on all nucleocapsids which lay entirely within their image fields and which appeared to be spatially separate from other particles or material. A total of 103 such measurements were made, yielding an average mass of 67.7 MDa but with a standard deviation of 14%, which is unexpectedly large (47). On closer examination, it became apparent that the initial data set had included some particles which were incomplete or had suffered partial loss of material, resulting in anomalously low mass values. Small pieces of obviously fragmented nucleocapsids were often seen in the vicinity of such particles (data not shown). In addition, some particles appeared to be compromised by residual salt deposits, and these gave anomalously high mass values. A total of 31 particles were rejected for these reasons. The remaining data, drawn from three independent and mutually consistent experiments (Table 1), gave a value of 69.4 ± 4.9 MDa for the nucleocapsid mass (i.e., ±7%). The distribution of these measurements (Fig. 5) was quite symmetrical, suggesting a homogeneous population.

Biochemical characterization of the protein contents of purified virions, pronase-treated virions, and nucleocapsids. Since interpretation of our STEM-determined masses in terms of protein stoichiometries is, to some extent, dependent on the use of biochemically well-defined samples, the purity of these preparations was assessed by SDS-PAGE.

(i) Purified virions. Figure 6a shows an SDS-PAGE profile of purified VSV grown in the presence of [^{3}H]leucine. It is apparent that only the five VSV proteins (L, G, NS, N, and M) were present in significant amounts. The molar ratios of the L, G, NS, and M proteins relative to N protein are reported in Table A1 (cf. Appendix).

(ii) Pronase-treated virions. Figure 6b shows the electrophoretic profile of the polypeptides of pronase-shaved virions. The molar ratios relative to N protein calculated for the M, G, L, and NS proteins were 1.49, 0.00, 0.03, and 0.33, respectively. Thus, only G protein was degraded since no significant change in the relative amounts of the other viral proteins was detected. The small peak of radioactivity found running ahead of M protein, which is not found in the control virus, is probably derived from G protein (38).

(iii) Nucleocapsids. The nucleocapsids used in these experiments were prepared from [^{3}H]leucine-labeled virus by a detergent–high-salt treatment (10). The protein composition of the nucleocapsid preparation is shown in Fig. 6c and Table 2. N protein was by far the major component; NS

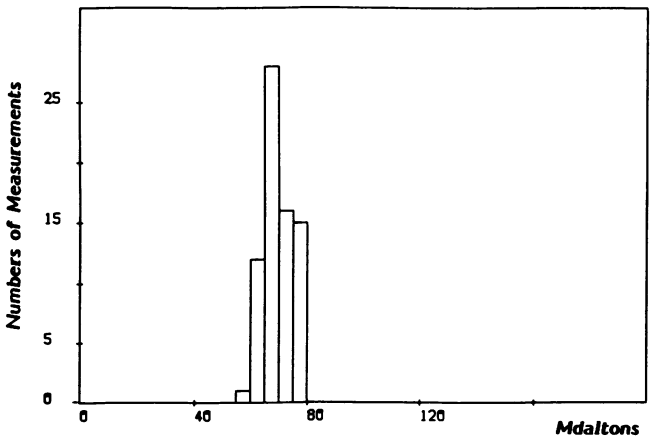

FIG. 5. Distribution of STEM mass measurements made on isolated nucleocapsids (n = 72). The histogram is symmetrical, suggesting a homogeneous population.

protein was present at about 40% of its relative abundance in virions; and only trace amounts of the M, G, and L proteins were detected.

Determination of the length of the VSV nucleocapsid. In addition to determining the mass of purified nucleocapsids, we also addressed the question of their total length. Such measurements by microscopy are potentially subject to various types of systematic error, such as measurements of broken or otherwise incomplete particles, uncertainties as to total contour length if the particle is not spread out in a fully extended configuration, or possible structural changes (e.g., stretching or shrinkage) which might be caused by the purification procedure or the preparation for electron microscopy. Accordingly, we employed four different methods to evaluate the nucleocapsid length.

(i) Determination from STEM measurements of mass per unit length and total mass. Unlike DNA heteroduplexes, for example, VSV nucleocapsids have a very pronounced tendency to coil up, so that images representing particles that appear convincingly to be totally spread out are rare; there were, in fact, none of these in our STEM data base. However, many particles show relatively short tracts where the nucleocapsid strand appears to be uniformly spread and to project a uniform density along the strand. By using such regions to perform local measurements (Fig. 4b), we obtained an average value of 22.7 ± 3.0 MDa/μm (n = 72) for the mass per unit length. Dividing the nucleocapsid mass (69.4 MDa) by this number yielded a value of 3.05 ± 0.5 μm for its length.

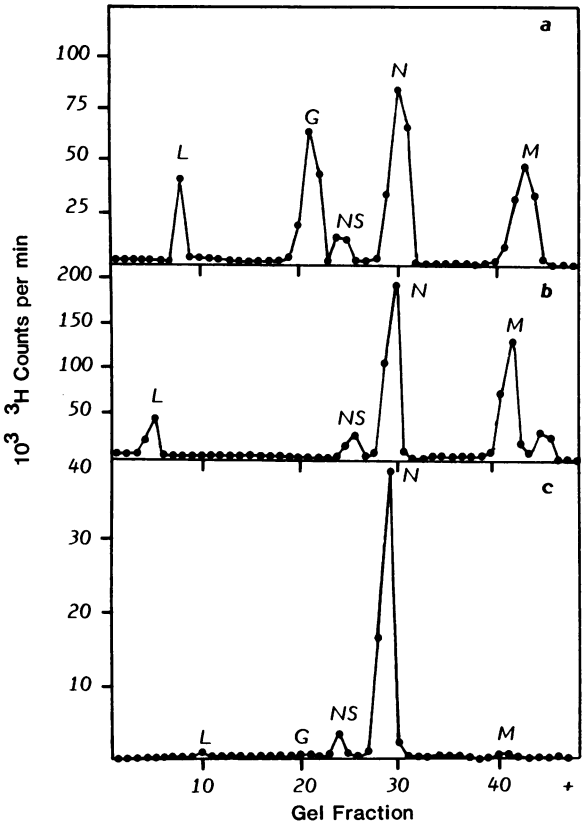

FIG. 6. SDS-PAGE data for VSV proteins labeled with [^{3}H]leucine: a, VS virions; b, pronase-treated virions; and c, isolated nucleocapsids. In purified virions, all five proteins of the VS virion (L, G, NS, N, and M) are present, whereas in pronase-treated virions, the G protein is absent. In isolated nucleocapsids, N protein is the major component (90.7% of total protein mass), and only trace amounts of the M, G, and L proteins are detected.

TABLE 2. Protein composition of isolated nucleocapsids expressed relative to N protein

Protein	Ratio relative to N protein:		
	cpm[a]	Molar	Mass
N	1.000	1.000	1.000
M	0.016	0.035	0.019
G	0.005	0.0054	0.006
L	0.010	0.0017	0.008
NS	0.052	0.131	0.069

[a] Derived from [^{3}H]leucine-labeled proteins as reported in Fig. 6c.

(ii) Contour length of extended, negatively stained nucleocapsids. With negatively stained preparations observed in the conventional electron microscope, images of nucleocapsids were obtained that appeared to be both well spread out and clearly separate from other particles, thus eliminating any ambiguity as to how many nucleocapsids may be involved in a given complex. A manual electronic digitizer was employed to trace the overall contour lengths of the particles. The resulting length was 3.7 ± 0.6 μm (n = 33) (Fig. 7).

(iii) Characterization of the structural repeat along the nucleocapsid strand. Examining negatively stained specimens by STEM, we obtained images which revealed the nucleocapsid substructure with particular clarity (Fig. 8). The width projected by the nucleocapsid strand varied considerably, from a maximum of ~9.0 nm to a minimum of ~4.5 nm. The nucleocapsid was seen to be composed of repeating asymmetrical units whose long axes are oriented perpendicular to the direction in which the strand runs. This repeating structure was also discernible, albeit less conspicuously, in the unstained freeze-dried specimens (Fig. 4). Moreover, a dark-staining groove which ran along the strand was clearly visible (Fig. 8, arrows) and appeared to be located near the center of the strand when the nucleocapsid was viewed so that it projected its greatest width.

The spacing of the repeating units along the strand was marked by pronounced transverse striations (Fig. 8). This periodicity was determined, after video display of the im-

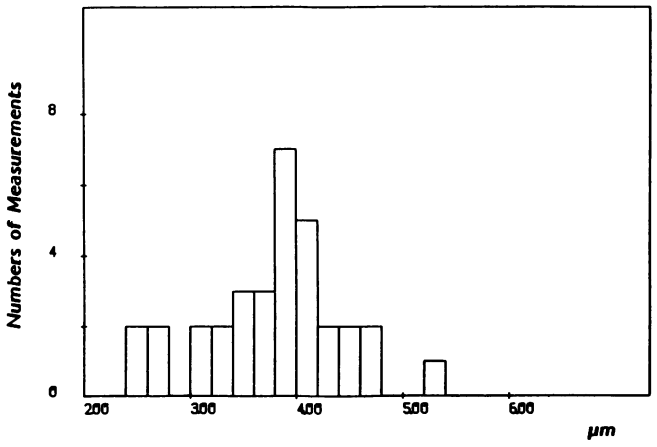

FIG. 7. Histogram showing the distribution of nucleocapsid lengths determined by measuring contour lengths from conventional transmission electron microscope images of negatively stained, well-extended specimens.

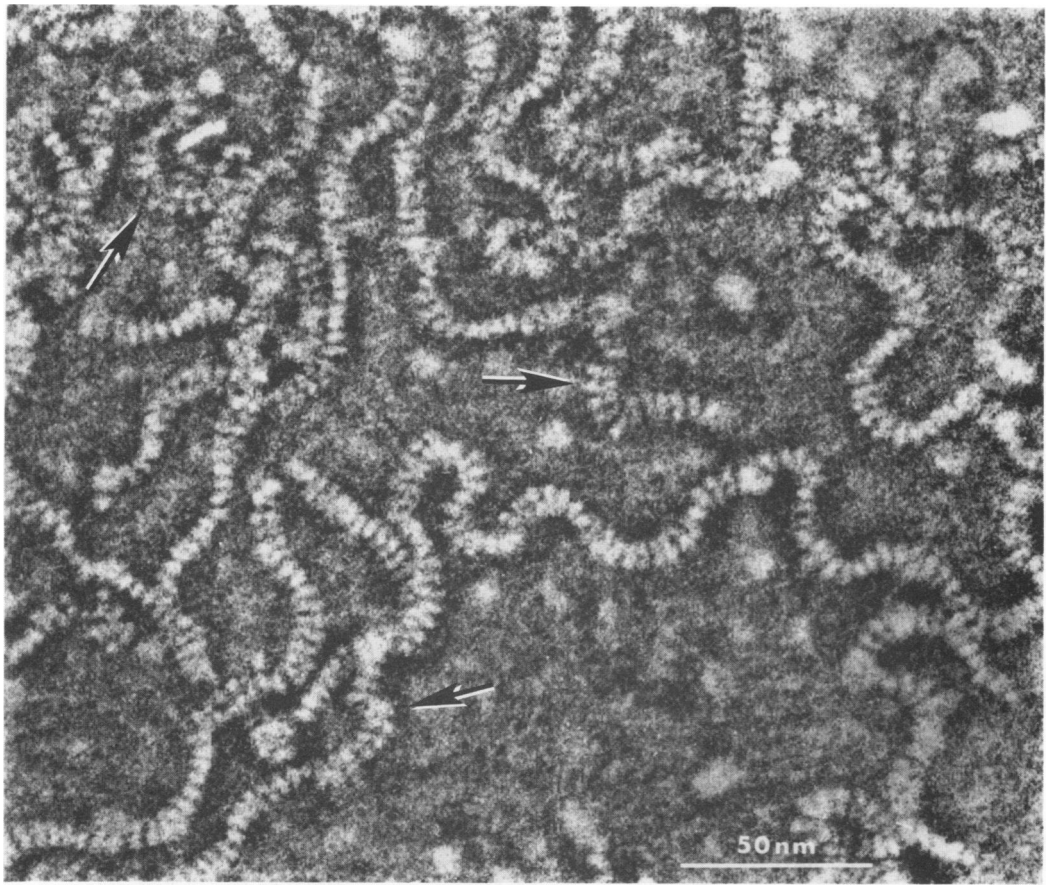

FIG. 8. STEM image of negatively stained VSV nucleocapsids. The widths of the ribbons vary (from ~9.0 to ~4.5 nm) according to their orientation on the support film. Structural units are clearly resolved, and in some places a dark-staining groove running parallel to the strand is visualized (arrows).

ages, by measuring the contour length along the center of the strand with a cursor and then counting the corresponding number of units. This procedure yielded a value of 3.3 ± 0.1 nm for the center-to-center distance, where each of the 25 measurements covered 5 to 10 repeats. Because the nucleocapsids appear to be entirely composed of such repeating units and because N protein is by far their major constituent, it is very likely that each unit contains an oligomer of N protein (of which we estimate there are 1,258 copies per nucleocapsid; see below). If the repeating unit represents a monomer of N protein, this would correspond to a nucleocapsid length of 4.1 μm. If a dimer is involved, the length would then be 2.05 μm, etc. In view of the other length measurements reported here, it seems very unlikely that the 3.3-nm repeat can represent anything other than a monomer of N protein. Accordingly, an estimate of 4.1 μm for the nucleocapsid length follows from this calculation.

(iv) Calculation of nucleocapsid length from in situ measurements. Longitudinal thin sections and negative staining of VS virions reveal prominent striations running approximately perpendicular to the particle axis with a repeat distance of ~5.0 nm (29, 30). This periodicity has been explained as the helical pitch of the coiled nucleocapsid packaged within the virion. Nakai and Howatson (29) have reported that there are 34 ± 2 such striations per virion, i.e., 34 coils of the helix (N). The total length (ℓ) of an N-coil helix with radius r and pitch p is given by the expression

$$\ell = 2\pi N[r^2 + (p^2/4\pi^2]^{1/2}.$$

By specific cytochemical staining for RNA (1), we have determined the radial location of the RNA from electron micrographs of transverse thin sections as r = 15 nm (D. Thomas, W. W. Newcomb, J. C. Brown, J. S. Wall, J. F. Hainfeld, B. L. Trus, and A. C. Steven, manuscript in preparation). If the length of the nucleocapsid is equated with that of the packaged RNA, a value of 3.2 ± 0.2 μm is given by the equation above for the length of the packaged nucleocapsid.

DISCUSSION

Mass of the VS virion. Our STEM mass determination experiments reproducibly yielded a value of 265.6 ± 13.3 MDa (Table 1) for the average particle mass of purified, morphologically intact virions. Previously, mass values have been calculated to be 290 ± 44 MDa (14) for VSV (Indiana) and 355 ± 45 MDa (48) for VSV (New Jersey) by combining diffusion coefficients evaluated by laser light scattering with sedimentation constants and partial specific volumes ($\bar{v}$). Within the limits of experimental error, the first evaluation is consistent with the present data, whereas the second is significantly higher. This discrepancy may reflect some difference between the Indiana and New Jersey strains. However, masses yielded by this method are acutely sensi-

tive to the value used for $\bar{v}$. Noting that a change in $\bar{v}$ from 0.78 (14) to 0.83 (48) is sufficient to account for the increased mass value, we suggest that uncertainty as to the value of this parameter is the primary reason for the inconsistently high mass given in the second report (48).

Molecular composition of the VS virion. The mass measurements and relative protein stoichiometries reported here can be employed in conjunction with the recently determined molecular weights of individual proteins (12, 35, 40) to calculate the complement of various molecular constituents of the virion.

(i) G protein. The virion mass was found to be reduced by 68.1 MDa after pronase digestion (Table 1). Biochemically, this treatment results in quantitative disappearance of G protein from gels without affecting the other viral proteins (Fig. 6). Structurally, this digestion corresponds to removal of the protruding spikes (Fig. 3) (23). The moiety of G protein which is located external to the membrane, its "external domain," has a molecular weight of 56,398 (cf. Appendix), which leads us to a value of 1,205 copies for the median viral content of G protein. Thus, the total mass of G protein present in the virion is, on average, 75.2 MDa, of which the carbohydrate moieties contribute 7.9 MDa (cf. Appendix).

When the viral content of G protein was calculated relative to N protein from our biochemical experiments (see below), we obtained a value of 830 copies. In an earlier biochemical study, Cartwright et al. (6) estimated 500 molecules per virion. Since it has been shown that the amount of G protein in a virion depends heavily upon the time after infection at which the virion matures (21), estimates of G protein content are comparable only for preparations that are identical in this respect. This was true for the samples examined in our STEM and biochemical experiments, so the discrepancy between them must have some other explanation. The underlying reason may well be that the biochemical quantitation reflects the average G protein content over a somewhat heterogeneous population of particles that includes immature virions with incomplete membranes and particles whose membranes were damaged during purification, whereas the STEM measurements were restricted to morphologically intact particles. Thus, we consider it likely that the systematically lower value of the biochemically based estimate reflects the incidence of incomplete membranes on a certain fraction of the particles.

Moreover, the present data indicate that variations in the number of G proteins per virion occur among seemingly intact particles (21). On comparing the variabilities encountered in the virion mass data (standard deviation, 13.3 MDa) and among the shaved virus particles (standard deviation, 8.5 MDa), we found that the latter population was distinctly more homogeneous (cf. Fig. 2a and b). Since these specimens were prepared for microscopy and subsequently analyzed in the same way (thus incurring the same experimental errors from these sources), it is plausible that the difference between their standard deviations reflects a limited variability in the number of G proteins per virion. Assuming that the two contributions to the net standard deviation of the virion mass data (namely, that of the number of G proteins per particle and that from other sources at the same level as for the shaved virions) combine in quadrature, we obtained an estimate of ±181 molecules for the standard deviation characteristic of the variability in the numbers of G protein per virion in our preparations (i.e., ~15%).

(ii) N protein. The mass of the purified nucleocapsid was determined to be 69.4 MDa. This includes N protein as well as the nucleic acid and residual amounts of other proteins (Fig. 6). The VSV genome contains 11,162 nucleotides (40). This value, in light of the known base composition (34), gives a mass of 3.74 MDa for the viral RNA. By quantitating the relative amounts of the proteins (Table 2) in light of their known molecular weights and amino acid sequences, we found that N protein accounts for 90.7% of the protein mass of the purified nucleocapsids. Since the molecular weight of N protein is 47,355 (12), this corresponds to 1,258 copies of N protein per nucleocapsid. Assuming no loss of N protein during preparation of the nucleocapsids, we determined the contribution of N protein to the virion mass to be 59.6 MDa.

Estimates given in the literature for the viral complement of N protein vary widely. Murphy and Harrison (27) give a value of 1,000 molecules from equating the repeating structural units of the nucleocapsid characterized electron microscopically by Nakai and Howatson (29) with N protein monomers (see above). They also mention a value of 2,000 to 2,300 molecules per virion that was derived from biochemical determinations. Numbers of 1,800 to 2,100 molecules are given in other reviews (15, 46). Cartwright et al. (6) obtained a value of 1,100 molecules from biochemical quantitations. Our STEM-based determination gave a value of 1,258 molecules, which is close to the result of Cartwright et al. (6) and the deduction based on the data of Nakai and Howatson (29). The standard deviation (7%) in our nucleocapsid mass measurements, which may in part reflect differing amounts of residual L and NS proteins associated with different particles, corresponds to 1-standard deviation limits of 1,170 and 1,346 for the number of N protein monomers.

We considered the possibility that purification of nucleocapsids may be accompanied by a partial loss of the amount of N protein in the viral particle but concluded that this is unlikely. If the virion contained as many as 2,000 molecules of N protein, then the relative stoichiometry data indicate that its mass should be 430 MDa (calculated for a protein contribution of 64% of the total virion mass [24]); this value is not compatible with our experimentally determined value of 265.6 ± 13.3 MDa.

Based on the number of nucleotides in the VSV genome and the viral content of N protein molecules, a value of 8.87 ± 0.43 was determined for the number of nucleotide bases per N protein monomer in the repeating unit of the nucleocapsid strand (see below). Assuming an integral stoichiometry, there are most likely nine nucleotides per monomer. Interestingly, this value correlates well with the properties of 5′ sequences of leader RNAs with a high affinity for N protein binding for which Blumberg et al. (4) identified a largely conserved 18-residue sequence with a strikingly high incidence of adenosine. This sequence appears to be an approximate duplication of a nine-base sequence and may therefore represent the sites which bind the first two molecules of N protein, thereby initiating assembly of the nucleocapsid.

(iii) M, NS, and L proteins. Our determinations of the relative stoichiometries of the M, NS, and L proteins in the virion, as evaluated by radioactivity counting on gels, are consistent with the values determined in other laboratories (see Table A1). Accordingly, we calculated the viral content of these proteins relative to the content of N protein. This procedure yielded values of 1,826 copies of M protein (47.6 MDa), 50 copies of L protein (12.1 MDa), and 466 copies of NS protein (11.7 MDa) per virion.

Table 3 summarizes the protein composition of the VS virion. Numerically, M protein is the most abundant protein

TABLE 3. Protein composition of the VS virion

Protein	No. of molecules per virion	Mass per virion in MDa (%)	% of total protein
G[a]	1,205	67.0	33.8
N	1,258	59.6	30.1
NS	466	11.7	5.9
L	50	12.1	6.1
M	1,826	47.6	24.0

[a] Polypeptide moiety of the G protein.

(1,826 copies) in the particle, whereas G protein makes the largest contribution to its mass.

(iv) Lipid content. The foregoing calculations yielded a total mass of 205.9 MDa per virion for protein and glycoprotein. If, apart from the RNA (3.7 MDa), the remaining mass is assumed to be accounted for by lipid in the viral envelope, then we obtain a value of 56 MDa for the lipid content, corresponding to 21.1% of the total mass of the virion. The lipid composition of VSV has been shown to consist predominantly of phospholipids (61%) and neutral lipids (39%), with a cholesterol-to-phospholipid molar ratio of 0.6 (24). The packing density of lipids within the membrane and the fraction of its area which is occupied by lipid are not clearly established. However, on the assumption that phospholipids and cholesterol are in a bilayer configuration, we can calculate a number of 4.5×10^4 molecules of phospholipid by using a value of 750 for the average molecular weight. Thus, the cholesterol-to-phospholipid ratio gives a number of 2.7×10^4 molecules of cholesterol per virion. If the shape of the viral membrane is approximated as a cylinder of 145 nm in length and 31.7 nm in radius terminated with hemispherical ends of the same radius (Fig. 3) to give a total length of 176.7 nm, this would correspond to a total membrane surface of 3.83×10^4 nm^2. Thus, we find a surface area of 0.9 nm^2 per lipid molecule in a bilayer configuration. This value is compatible with corresponding values calculated for synthetic bilayers (~0.8 nm^2) (8, 36).

(v) Chemical composition of VSV. The foregoing calculations afford a quantitative account of the chemical composition of the VS virion (Table 4). These values are in reasonable overall agreement with the chemical analysis of McSharry and Wagner (24), particularly with respect to protein and lipid content.

Structure of the VSV nucleocapsid. (i) Length of the nucleocapsid. The nucleocapsid length was evaluated by four different methods, each of which is potentially subject to different sources of systematic and random error. Thus, the reasonable measure of agreement obtained engenders confidence in the results. From these data, we conclude that the length of the intact VSV nucleocapsid is 3.5 to 3.7 μm, and we discuss below the limited variation (3.1 to 4.1 μm) encountered among the various measurements.

A length of 3.1 ± 0.5 μm was obtained from STEM determinations of the nucleocapsid mass and its mass per unit length. Here the major source of error lies in the average mass-per-unit length determination from measurements performed on relatively short segments that appeared to be evenly spread. However, these segments may not lie uniformly flat in the plane of the carbon film substrate. It is possible that in some cases these strands may loop away from the support film so that their apparent projected length is an underestimate because of foreshortening. This effect would bias the mass-per-unit length measurement to a higher value which, in the present context, would be reflected in an underestimate of the nucleocapsid length. Thus, although in view of the estimated random error (±0.5 μm) this determination (3.1 μm) is not inconsistent with our favored value of 3.5 to 3.7 μm, the slight difference may well be due to this foreshortening effect.

Integration of the in situ length of the coiled nucleocapsid visualized in intact virions gave an estimate of 3.3 μm. It is not straightforward to assess a margin of error for this determination which depends, among other factors, on the number of helical coils, which is taken to be 34 ± 2 (29). However, we consider it unlikely to be an overestimate since there may be additional portions of nucleocapsid at its extremities which are not organized in coils.

Contour length measurements of negatively stained nucleocapsids in extended configuration yielded a value of 3.7 ± 0.6 μm. This value and the substantial standard deviation are consistent with the earlier measurements made using this technique by Nakai and Howatson (29).

A value of 4.1 ± 0.3 μm was obtained by combining a determination of the linear repeat along the nucleocapsid strand (3.3 ± 0.1 nm) with the number of N protein monomers deduced from STEM mass determinations. This length appears to be on the high side of our favored value, although not by a margin that significantly exceeds the estimated margin of error. However, it should be noted that, even when extended, the nucleocapsid usually shows pronounced curvature (Fig. 4 and 8). The strand width when flat is approximately 9.0 nm, and the radius of curvature of the strand at the inner side is of the same order of magnitude. Consequently, the value of the repeat distance depends upon the location between the inner (concave) and outer (convex) sides of the strand at which the measurement is made. The structural repeat is most prominent at the outer edge (Fig. 8), and our measurements apply to the middle of the strand, although other choices are possible. This ambiguity may underlie the slight disparity between this determination and our concluded value.

(ii) Structure of the nucleocapsid subunit. In their electron microscopy study of VSV structure, Nakai and Howatson (29) proposed a model for the repeating units of the nucleocapsid (which we have shown to represent N protein monomers) as rods with dimensions of 3.0 by 3.0 by 8.0 to 10.0 nm. Our observations on negatively stained nucleocapsids are in general agreement with these findings, but they differ in certain particulars. From the images obtained in this study, we measured values of ~9.0 and ~4.5 nm for the maximum and minimum widths projected by the negatively stained nucleocapsid strands, which correspond to the length and the thickness of its subunits, respectively. Our length determination is consistent with that of Nakai and Howatson (29), but our value for the thickness is significantly greater. In this respect, electron microscopy observations on negatively stained and thin-sectioned virions (29, 30, 41) have shown that the pitch of the helically coiled intraviral nucleocapsid is 4.6 to 5.0 nm. This dimension is imposed by the thickness of the subunit, which may in fact be somewhat

TABLE 4. Chemical composition of VSV

Component	Mass (MDa)	Mass (%)
Protein	198.0	74.5
Lipid	56.0	21.1
Carbohydrate	7.9	3.0
Nucleic acid	3.7	1.4

TABLE A1. Stoichiometry of the VSV proteins expressed relative to N protein

Protein	[^{3}H]leucine cpm ratio		Molar ratio from data of study[a]:		
	Expt. 1	Expt. 2	A	B	C
N	1.00	1.00	1.00	1.00	1.00
M	0.66	0.68	1.50	1.43	1.45
G	0.67	0.54	0.66	0.50	0.51
L	0.21	0.22	0.037	0.041	0.043
NS	0.12	0.12	0.30	0.38	0.38

[a] A, Present study; B, primary data (cpm ratio) taken from Pinney and Emerson (32) and converted to molar ratio; C, J. Wiener (personal communication).

greater should there be appreciable intercalation between the subunits in successive layers.

In the images we obtained (e.g., Fig. 8), when the nucleocapsid ribbon is viewed so that the subunits project their long axes, they appear to be distinctly wedge shaped, with a width at their midpoint corresponding to our measured center-to-center repeat of 3.3 nm. Moreover, the dark-staining groove visualized along the middle of the strand (Fig. 8, arrows) strongly suggests that the subunit is bilobed. Thus, we propose that the N protein subunit in the nucleocapsid has a wedge-shaped, bilobed structure: this property can explain the characteristic undulating configuration assumed by the nucleocapsid even when the strand is well extended.

APPENDIX

Molecular weights of G protein and its moieties. The molecular weight of G protein was considered to be the sum of contributions from its amino acid sequence, two carbohydrate moieties, and one palmitic acid group. The external domain was considered to be that part of the molecule distal to its transmembrane moiety.

As predicted from the mRNA sequence (35), the amino acid sequence of G protein is 511 amino acids long, with a calculated molecular weight of 57,416. This includes the NH_2-terminal "signal" sequence of 16 amino acids not present on the mature protein, so the molecular weight of the polypeptide moiety of mature G protein (495 amino acids) is 55,587. The hydrophobic moiety which spans the membrane is 20 residues in length and is followed at the CO_2 terminus by a hydrophilic sequence of 29 amino acids, which is located inside the viral envelope (35). Thus, the external domain which protrudes from the viral envelope comprises 446 amino acids and has a molecular weight of 49,962.

G protein contains two identical carbohydrate chains, each composed of one molecule of fucose, three of mannose, three of galactose, five of *N*-acetylglucosamine, and three of *N*-acetylneuraminic acid (33). Thus, the polysaccharide moiety of G protein has a predicted mass of 6,528. The G protein also contains one palmitate group (molecular weight 239) located on the cytoplasmic side of the virus membrane (39). Accordingly, the total molecular weight of the mature glycoprotein is 62,354, and its external domain has a molecular weight of 56,398, corresponding to 90.5% of the total.

TABLE A2. Molecular weights and leucine contents of VSV proteins

Protein	Mol wt	Leucine residues	Reference
N	47,355	38	12
M	26,064	17	35
G	55,587[a]	35	35
L	241,012	219	40
NS	25,110	15	12

[a] Molecular weight of the polypeptide moiety.

Relative amounts of the N, M, L, NS, and G proteins: determination by radiolabeling. Biochemical estimates of the relative abundances of the N, NS, M, L, and G proteins have been made in several studies in which these proteins were radiolabeled with [^{3}H]leucine. Some representative results are compiled in Table A1. The respective counts have been converted into molar and mass ratios (relative to the amount of N protein in each case) by using recently determined primary sequence data for these proteins (Table A2) (12, 35, 40). No corrections were applied for possible effects of differing amino acid pool sizes or for metabolic transfer of the label to other amino acids.

ACKNOWLEDGMENTS

We thank N. Crowe for software contributions, K. Cheung, N. Salomonsky, and F. Kito for expert technical assistance, B. Morille for photography, and D. E. Chunko for preparing the manuscript.

This study was partly supported by Public Health Service grant GM-34036 (to J.B.) and Biotechnology Resources grant RR-01777 (to J.W. and J.H.) from the National Institutes of Health.

LITERATURE CITED

1. **Bernhard, W.** 1969. A new staining procedure for electron microscopical cytology. J. Ultrastruct. Res. **27**:250–265.
2. **Bishop, D. H. L., and M. Smith.** 1977. Rhabdoviruses, p. 167–280. *In* D. Nayak (ed.), The molecular biology of animal viruses, vol. 1. Marcel Dekker, Inc., New York.
3. **Bishop D. H. L., and P. Roy.** 1972. Dissociation of vesicular stomatitis virus and relation of the virion proteins to the viral transcriptase. J. Virol. **10**:234–243.
4. **Blumberg, B. M., C. Giorgi, and D. Kolakofsky.** 1983. N-protein of vesicular stomatitis virus selectively encapsidates leader RNA in vitro. Cell **32**:559–567.
5. **Carroll, A. R., and R. R. Wagner.** 1978. Inhibition of transcription by immunoglobulins directed against the ribonucleoprotein of homotypic and heterotypic vesicular stomatitis viruses. J. Virol. **25**:675–684.
6. **Cartwright, B., C. J. Smale, F. Brown, and R. Hull.** 1972. Model for vesicular stomatitis virus. J. Virol. **10**:256–260.
7. **Cartwright, B., P. Talbot, and F. Brown.** 1970. The proteins of biologically active subunits of vesicular stomatitis virus. J. Gen. Virol. **7**:267–272.
8. **Cornell, B. A., J. Middlehurst, and F. Separovic.** 1980. The molecular packing and stability within highly curved phospholipid bilayers. Biochim. Biophys. Acta **598**:405–410.
9. **Crewe, A.** 1983. High resolution scanning transmission electron microscopy. Science **221**:325–330.
10. **Emerson, S. U., and R. R. Wagner.** 1973. L protein requirement for in vitro RNA synthesis by vesicular stomatitis virus. J. Virol. **12**:1325–1335.
11. **Engel, A.** 1978. Molecular weight determination by scanning transmission electron microscopy. Ultramicroscopy **3**:273–281.
12. **Gallione, C. J., J. R. Greene, L. E. Iverson, and J. K. Rose.** 1981. Nucleotide sequences of the mRNA's encoding the vesicular stomatitis virus N and NS proteins. J. Virol. **39**:529–535.
13. **Hainfeld, J. F., J. S. Wall, and E. J. Desmond.** 1982. A small computer system for micrograph analysis. Ultramicroscopy **8**:263–270.
14. **Hartford, S. L., J. A. Lesnaw, W. H. Flygare, R. MacLeod, and M. E. Reichmann.** 1975. Physical properties of New Jersey serotype of vesicular stomatitis virus and its defective particles. Proc. Natl. Acad. Sci. U.S.A. **72**:1202–1205.
15. **Heyward, J., B. Holloway, P. Cohen, and J. Obijeski.** 1980. Rhabdovirus nucleocapsid, p. 137–150. *In* D. Bishop (ed.), Rhabdoviruses, vol. I. CRC Press, Inc., Boca Raton, Fla.
16. **Hunt, D. M., and R. R. Wagner.** 1975. Inhibition by aurintricarboxylic acid and polyethylene sulfonate of RNA transcription of vesicular stomatitis virus. J. Virol. **16**:1146–1153.
17. **Hunt, R., and J. Brown.** 1974. Surface glycoproteins of mouse L cells. Biochemistry **13**:22–28.
18. **Lamvik, M. K.** 1978. Muscle thick filament mass measured by electron scattering. J. Mol. Biol. **122**:55–68.

19. **Lenard, J.** 1978. Virus envelopes and plasma membranes. Annu. Rev. Biophys. Bioeng. **7**:139–165.
20. **Lenard, J., and R. Compans.** 1974. The membrane structure of lipid-containing viruses. Biochim. Biophys. Acta **344**:51–94.
21. **Lodish, H. F., and M. Porter.** 1980. Heterogeneity of vesicular stomatitis virus particles: implications for virion assembly. J. Virol. **33**:52–58.
22. **McSharry, J.** 1980. The lipid envelope and chemical composition of rhabdoviruses, p. 107–118. *In* D. Bishop (ed.), Rhabdoviruses, vol. I. CRC Press, Inc., Boca Raton, Florida.
23. **McSharry, J. J., R. W. Compans, and P. W. Choppin.** 1971. Proteins of vesicular stomatitis virus and of phenotypically mixed vesicular stomatitis virus-simian virus 5 virions. J. Virol. **8**:722–729.
24. **McSharry, J. J., and R. R. Wagner.** 1971. Lipid composition of purified vesicular stomatitis viruses. J. Virol. **7**:59–70.
25. **Mosesson, M. W., J. Hainfeld, R. H. Haschemeyer, and J. Wall.** 1981. Identification and mass analysis of human fibrinogen molecules and their domains by scanning transmission electron microscopy. J. Mol. Biol. **153**:695–718.
26. **Mudd, J.** 1974. Glycoprotein fragment associated with vesicular stomatitis virus after proteolytic digestion. Virology **62**:573–577.
27. **Murphy, F. A., and A. K. Harrison.** 1980. Electron microscopy of the rhabdoviruses of animals, p. 65–106. *In* D. Bishop (ed.), Rhabdoviruses, vol. I. CRC Press, Inc., Boca Raton, Fla.
28. **Nagpal, M., and J. Brown.** 1980. Protein and glycoprotein components of phagosome membranes derived from mouse L cells. Int. J. Biochem. **11**:127–138.
29. **Nakai, T., and A. F. Howatson.** 1968. The fine structure of vesicular stomatitis virus. Virology **35**:268–281.
30. **Newcomb, W. W., and J. C. Brown.** 1981. Role of the vesicular stomatitis virus matrix protein in maintaining the viral nucleocapsid in the condensed form found in native virions. J. Virol. **39**:295–299.
31. **Newcomb, W. W., G. J. Tobin, J. J. McGowan, and J. C. Brown.** 1982. In vitro reassembly of vesicular stomatitis virus skeletons. J. Virol. **41**:1055–1062.
32. **Pinney, D. F., and S. U. Emerson.** 1982. In vitro synthesis of triphosphate-initiated *N*-gene mRNA oligonucleotides is regulated by the matrix protein of vesicular stomatitis virus. J. Virol. **42**:897–904.
33. **Reading, C. L., E. E. Penhoet, and C. E. Ballou.** 1978. Carbohydrate structure of vesicular stomatitis virus glycoprotein. J. Biol. Chem. **253**:5600–5612.
34. **Repik, R., and D. H. L. Bishop.** 1973. Determination of the molecular weight of animal RNA viral genomes by nuclease digestions. I. Vesicular stomatitis virus and its defective T particle. J. Virol. **12**:969–983.
35. **Rose, J. K., and C. J. Gallione.** 1981. Nucleotide sequences of the mRNA's encoding the vesicular stomatitis virus G and M proteins determined from cDNA clones containing the complete coding regions. J. Virol. **39**:519–528.
36. **Rothman, J. E., and D. M. Engelman.** 1972. Molecular mechanism for the interaction of phospholipid with cholesterol. Nature (London) New Biol. **237**:42–46.
37. **Ruigrok, R. W. H., P. J. Andree, R. A. M. HooftVan Huysduynen, and J. E. Mellema.** 1984. Characterization of three highly purified influenza virus strains by electron microscopy. J. Gen. Virol. **65**:799–802.
38. **Schloemer, R. H., and R. R. Wagner.** 1975. Association of vesicular stomatitis virus glycoprotein with virion membrane: characterization of the lipophilic tail fragment. J. Virol. **16**:237–249.
39. **Schmidt, M., and M. Schlessinger.** 1979. Fatty acid binding to the VSV glycoprotein: a new type of post-translational modification of the viral glycoprotein. Cell **17**:813–819.
40. **Schubert, M., G. G. Harmison, and E. Meier.** 1984. Primary structure of the vesicular stomatitis virus polymerase (*L*) gene: evidence for a high frequency of mutations. J. Virol. **51**:505–514.
41. **Simpson, R. W., and R. E. Hauser.** 1966. Structural components of vesicular stomatitis virus. Virology **23**:654–677.
42. **Smith, P. R.** 1978. An integrated set of computer programs for processing electron micrographs of biological structures. Ultramicroscopy **3**:153–160.
43. **Steven, A. C., J. F. Hainfeld, J. S. Wall, and C. J. Steer.** 1983. Mass distribution of coated vesicles isolated from liver and brain: analysis by scanning transmission electron microscopy. J. Cell. Biol. **97**:1714–1723.
44. **Steven, A. C., J. Wall, J. Hainfeld, and P. M. Steinert.** 1982. Structure of fibroblastic intermediate filaments: analysis by scanning transmission electron microscopy. Proc. Natl. Acad. Sci. U.S.A. **79**:3101–3105.
45. **Trus, B. L., and A. C. Steven.** 1981. Digital image processing of electron micrographs: the PIC system. Ultramicroscopy **6**:383–386.
46. **Wagner, R.** 1975. Reproduction of rhabdoviruses, p. 1–93. *In* H. Frankel-Conrat and R. Wagner (ed.), Comprehensive virology, vol. 4. Plenum Publishing Corp., New York.
47. **Wall, J.** 1979. Mass measurements with the electron microscope, p. 333–342. *In* J. Hren, J. Goldstein, and D. Joy (ed.), Introduction to analytical electron microscopy. Plenum Publishing Corp., New York.
48. **Ware, B. R., T. Raj, W. H. Flygare, J. A. Lesnaw, and M. E. Reichmann.** 1973. Molecular weights of vesicular stomatitis virus and its defective particles by laser light-scattering spectroscopy. J. Virol. **11**:141–145.